Int. J. Heat Mass Transfer. Vol. 32, No. 8, pp. 1517–1527, 1989
Printed in Great Britain

0017–9310/89 $3.00+0.00

An experimental study of heat transfer in a vertical annulus with a rotating inner cylinder

K. S. BALL,† B. FAROUK and V. C. DIXIT

Department of Mechanical Engineering and Mechanics, Drexel University, Philadelphia, PA 19104, U.S.A.

(*Received* 25 *August* 1988 *and in final form* 6 *January* 1989)

Abstract—The results of an experimental study of the convective flows engendered within the annular gap between concentric vertical cylinders are presented. The inner cylinder is rotating and heated, while the outer cylinder is stationary and cooled. Stationary horizontal endplates are used to seal the annulus, forming an enclosure. The working fluid is air. Of particular interest is the accurate prediction of the heat transfer rates, which are intimately linked to the structure of the flow field. In rotating systems, the existence of hydrodynamic instabilities may lead to a variety of secondary flows as the parameters describing the system are varied. Along with each transition in a flow, the transport mechanisms are altered, and usually result in markedly changed rates of heat and momentum transport. Experiments are conducted to determine the interdependence between the heat transfer mechanism and the structure of the secondary flows. Specifically, a parametric study of the mean heat transfer rate across the annular gap is performed, as well as a qualitative study (using smoke visualization techniques) of the secondary flow characteristics of the rotating system. The results provide a qualitative description of the transition from a buoyancy-dominated flow regime to one dominated by rotation. A correlation for the heat transfer rate as a function of the rotational Reynolds number and radius ratio is obtained in the forced convection limit.

INTRODUCTION

HEAT AND mass transfer from rotating cylindrical bodies occurs in many practical applications, the most common being the cooling of conventional rotating machinery, such as electrical motors and turbines [1]. The development of new rotating devices has further stimulated interest in this area. Among these are clinical blood oxygenators [2], gas centrifuges [3], and 'barrel reactors' used in the chemical vapor deposition (CVD) process [4]. Also, rotating heat exchangers operating in a variety of different ways are being introduced in the chemical, automotive, and nuclear industries. Buoyant rotating flows also occur in nature (e.g. oceanic and atmospheric circulation), and provide useful models for study [5].

In spite of its technological importance, little work has been directed toward the study of heat transfer within rotating cylindrical annuli. The isothermal flow configuration, in contrast, has been the subject of much research. It is widely known that a critical speed of rotation exists, above which appears a stable, secondary mean flow consisting of regularly spaced toroidal vortices. This flow is commonly referred to as Taylor–Couette or Taylor-vortex flow, and results from an inherent hydrodynamic instability. A comprehensive review of the general Taylor problem is provided by DiPrima and Swinney [6]. A considerable amount of research has also been conducted for the natural convection problem (with no rotation). The recent paper by Weidman and Mehrdadtehranfar [7] investigates the stability of the natural convection flow in a tall annulus using the flow visualization technique, and also provides a good review of previously published results.

The first efforts to study the combined problem with rotation and heat transfer were primarily experimental, and were usually coupled with an axial flow through the annular gap [8–14]. Global heat transfer rates across the annular gap were reported, corresponding to the different flow regimes which were observed. However, these studies were limited to the forced convection regime, and no effort was made to quantify the magnitude of the buoyancy effects (such as reporting values of the cylinder surface temperatures or the Grashof number). Furthermore, the role of the radius ratio as a parameter in this problem was neglected, and therefore some discrepancies between the heat transfer measurements in the studies cited above could not be explained.

Later theoretical studies focused on the stability of the circular Couette flow in the presence of a radial temperature gradient [15–17]. With the inner cylinder rotating, it was concluded that a positive gradient of temperature across the annular gap (i.e. a heated outer cylinder and a cooled inner cylinder) is destabilizing, while a negative temperature gradient is stabilizing. This can be explained by noting that a greater centrifugal force is exerted on a heavier (cooler) fluid particle. Thus, fluid particles adjacent to a cooled inner cylinder would have a greater tendency to be displaced by the rotating flow. In these analyses, the gravity force (buoyancy) was neglected. Walowit *et al.* [17] justified this seemingly severe restriction by noting that in the conduction regime ($Gr \leqslant 10^3$), natural convection has little effect on the heat transfer, and

†Present address: Division of Applied Mathematics, Brown University, Providence, RI 02912, U.S.A.

NOMENCLATURE

d	gap width, $R_o - R_i$	ΔT	temperature difference across gap, $T_i - T_o$
g	acceleration due to gravity	V	voltage supplied to inner cylinder heater
Gr	Grashof number, $d^3\beta g\Delta T/\nu^2$	z	axial coordinate.
h	convection heat transfer coefficient		
H	height of annulus		
k	wave number, or thermal conductivity	Greek symbols	
k_{eq}	local equivalent conductivity, $hR \ln R_o/R_i/k = -hR \ln(\eta)/k$	β	thermal coefficient of volumetric expansion
R_i	inner cylinder radius	Γ	aspect ratio, H/d
R_o	outer cylinder radius	η	radius ratio, R_i/R_o
r	radial coordinate	ν	kinematic viscosity
Re	rotational Reynolds number, $(R_i\Omega)d/\nu$	σ	densiometric Froude number, Gr/Re^2
T_i	mean inner cylinder temperature	Ω	angular speed of rotation of inner cylinder.
T_o	mean outer cylinder temperature		

can therefore be expected to have little effect on the stability of the flow. However, Snyder and Karlsson [18–20] concluded that the axial flow induced by buoyancy does, in fact, have a significant influence on the stability of the flow. They found that both positive and negative radial gradients of temperature are stabilizing, provided that the magnitude of ΔT is small. For larger ΔT, a spiral form of instability was observed. More recent experimental studies have also confirmed the stabilizing effects of a positive density gradient [21, 22].

Numerical studies have also been reported in the literature for the mixed convection flows in a rotating annulus. These are discussed in refs. [23–26], in which the effects of buoyancy on the development of the Taylor-vortex flow are considered. The present paper is the experimental complement to those numerical studies.

EXPERIMENTAL FACILITY

The experimental facility used to study the mixed convection flows within the vertical annulus is designed to encompass as wide a range of the relevant parameters as possible, so that a systematic investigation of the effects of both the buoyancy and the centrifugal forces on the overall flow stability and concomitant transport mechanisms can be accomplished. Specifically, it is desired to determine the quantitative effects of varying the Grashof number Gr (which characterizes the buoyancy force) and the Reynolds number Re (which characterizes the centrifugal force) on the mean equivalent conductivity k_{eq}. The rotational parameter $\sigma \equiv Gr/Re^2$ indicates the relative importance of the buoyancy and rotational effects. These effects are of comparable magnitude for values of σ near unity, and consequently σ is used to delineate the different flow regimes in this study. The physical dimensions of the annulus were chosen so that values of σ ranging from $0.01 < \sigma < \infty$ could be obtained with reasonably moderate speeds of rotation and electrical heating power. Prandtl number effects are not considered in this study.

A schematic diagram showing the major components of the annular facility is shown in Fig. 1. The individual components can be loosely divided into three main subsystems: the actual test section, the supports and drive mechanism, and the slip ring assembly. Each of these subsystems will be described below.

The test cylinders used in this study were manufactured from commercial aluminum tube stock. Three different outer cylinders, with inner diameters of 5.725, 4.432, and 3.816 cm are employed. An

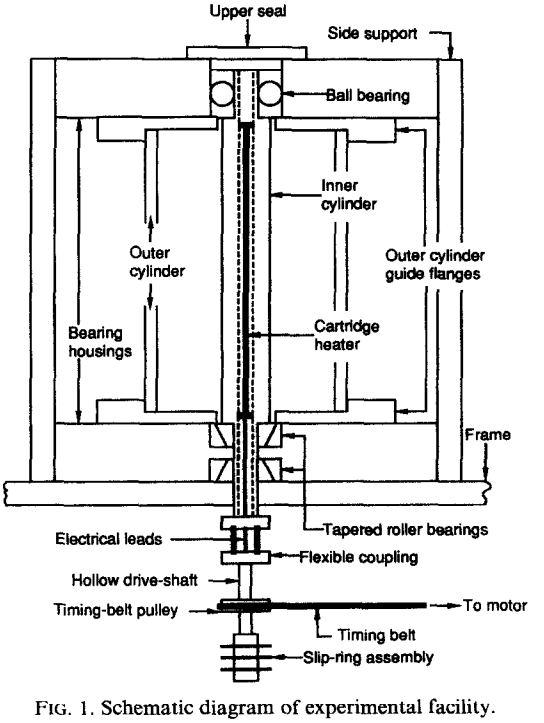

FIG. 1. Schematic diagram of experimental facility.

additional outer cylinder was constructed of plexiglas for use in the flow visualization studies, with a nominal inner diameter of 5.715 cm. Due to the substantial machining requirements of the inner cylinder, only one was constructed and is used with each of the outer cylinders. The final outside dimension of the inner cylinder is 2.504 cm. The length of the annular test section is 50.64 cm in all cases. Thus, for the quantitative heat transfer studies, the first facility has a radius ratio (inner to outer cylinder) of $\eta = 0.437$ and an aspect ratio (height to gap width) of $\Gamma = 31.44$, while for the second facility $\eta = 0.565$ and $\Gamma = 52.53$, and $\eta = 0.656$ and $\Gamma = 77.20$ for the third.

There are several reasons for designing a facility with relatively large aspect ratios. The most important of these is to provide a large enough heat transfer surface so that the power supplied to the electrical heater can be measured accurately. Also, the importance of the end effects associated with a finite geometry can be minimized. Finally, the larger cylinders are easier to work with during the machining process and construction of the facility. It is noted that the aspect ratio is expected to have little effect on the quantitative behavior of the flow for aspect ratios above $\Gamma = 40$ [27]. In this range of Γ, the radius ratio is the only geometrical parameter observed to have a significant influence on the flow.

The inner cylinder is heated by a 650 W cartridge heater. The heater is supported in the center of the test-section area by threaded metal plugs, which are screwed into the inner diameter of the cylinder. The heating power is provided by a d.c. power supply, and is varied through the use of a rheostat. The voltage and current are measured by two digital multimeters.

The outer cylinder is mounted between two flanges, which have guides counterbored in them to ensure that the two cylinders are concentric. The flanges also serve as seals for the annulus, as the clearance between the inner cylinder and each flange is 0.025 cm. The outer cylinder is cooled by passing an ethylene glycol–water mixture through a flexible plastic hose which is coiled around it. The entire arrangement is encased within a foam rubber insulating pad. Two thermocouples are sealed within the plastic tubing to measure the temperature of the coolant at both the entrance and exit to the coiled section. The cooling solution is maintained at a constant temperature by a refrigerated circulating unit manufactured by PolyScience, Inc., Niles, Illinois. The unit has a 1/6 hp compressor and a 1000 W heater, which are operated against each other by a proportional controller, allowing for a variation in bath temperature of less than ± 0.1°C. With this arrangement, the outer cylinder could be held isothermal to within ± 1.0°C.

The surface temperatures of both the inner and outer cylinders are measured by thermocouples imbedded within the cylinder walls. Five thermocouples are used to measure the outer cylinder temperature at various axial locations, while a total of seven thermocouples are used in the inner cylinder. An additional thermocouple is used to measure the ambient room temperature. All of the electrical connections to the rotating inner cylinder are made through the use of a high-precision slip-ring assembly manufactured by Industrial Electric Reels, Inc., Omaha, Nebraska.

The test cylinder is rotated by a 90 V, 1/4 hp, permanent magnet d.c. motor. A timing-belt system is used to achieve the transfer of torque to the cylinder. Timing belts allow for very quiet operation at constant rates of speed, with no slippage at lower velocities. A solid-state silicon-controlled rectifier (SCR) is used to vary the speed of rotation. The motor is capable of driving the cylinder at speeds of up to 1735 r.p.m. For rotational speeds below approximately 120 r.p.m., the motor is used in conjunction with a worm-gear speed reducer to minimize any variations in the speed. With this arrangement, constant rotational speeds of as low as 1 r.p.m. can be achieved. The drive shaft is connected to the inner cylinder by a flexible coupling, virtually eliminating any alignment problems or the transmission of vibrations to the test cylinder.

Data acquisition system

In conjunction with the design of the experimental facility, a general purpose microprocessor-based data acquisition system was developed. The data acquisition system is centered around an Apple IIe microcomputer, and was assembled at about the same cost as a single, commercially available, one-function data-logging device. The computer is equipped with a real-time clock (purchased from Thunderware, Inc., Oakland, California) which is used as an event timer, triggering scans at any desired time or at preselected time intervals. Data can either be reduced and printed out in real time or stored on diskettes for later processing.

For the purpose of measuring temperatures, a single-board microprocessor-controlled measurement system (Omega Engineering, Inc., Stamford, Connecticut, μMEGA 4000) is used, which can accept up to 12 thermocouple inputs. It is connected to the Apple IIe through a serial interface. This device provides preamplification, scaling, and automatic multiplexing of the thermocouple input signals. Several types of thermocouples can be used. All conversions to engineering units, cold-junction compensation, linearization, and data output formatting are performed by the measurement system. For type T thermocouples (copper–constantan), a resolution of 0.1°C is obtained. Further details regarding the data acquisition system can be found in ref. [28].

Flow visualization system

For the visualization studies, a smoke generation system was developed, in which a light petroleum solution is rapidly heated to produce a dense white oil fog. Commercially available smoke solutions, sold by hobby shops for model locomotives, etc., were found to be ideally suited for this purpose. A schematic of

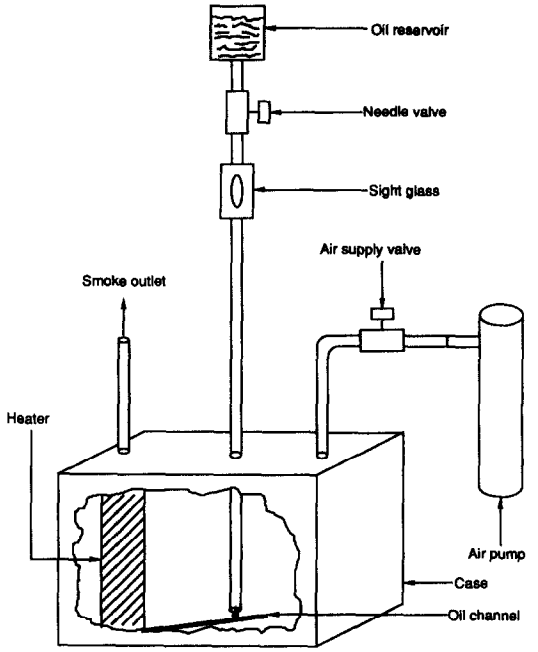

FIG. 2. Schematic diagram of flow visualization system.

the smoke-generating unit is shown in Fig. 2. In this unit, oil is allowed to drip from a reservoir through a tube and onto a small gutter, which directs the oil droplets to the heating surface. The droplet flow rate is controlled by a needle valve. The unit is tightly sealed, with two openings provided for a forced-air flow which is used to carry the smoke to the test section.

The smoke is injected into the test section through a small plastic tube. One end of this tube is inserted into a port which was drilled into the wall of the plexiglas outer cylinder. The other end of the tube is connected to the smoke outlet, where a valve can be used to control the flow of the smoke. In operation, a small amount of smoke is injected into either the top or the bottom of the annulus. As the smoke gradually diffuses into the interior of the annulus, the cellular flow patterns (if present) become visible. The flow is illuminated by a thin plane of light, which is produced by enclosing a long fluorescent lamp within a box that has a thin slit cut into one of its sides. The photographs are taken with a 35 mm SLR camera, using Ilford XP-1 film, which has a variable film speed that is ideally suited for low light applications. The camera is mounted on a tripod. Between successive pictures, the annulus is purged with fresh air and allowed to settle.

Operation

Three quantities can be varied independently in this system: the speed of rotation of the inner cylinder, the temperature of the cooling bath, and the voltage applied to the inner cylinder heater. For a given combination of these parameters, the temperature of the inner cylinder will eventually reach a certain fixed value. When this value is obtained, the system is in a state of equilibrium. This condition is ascertained by measuring the inner cylinder temperature at selected time intervals and observing any changes. When these changes become small (within $\pm 0.1°C$), the steady-state condition is assumed. For every case studied, the equilibration time was approximately 1 h. To be certain that the values recorded are representative of the steady-state condition, measurements are extended for at least a further 1 h beyond the transient settling period, and the average of these values is used in the subsequent calculations.

PROCESSING OF DATA

The Grashof number Gr and the Reynolds number Re (which are defined in the Nomenclature) can be calculated directly from the raw data set $\{T_o, V, \Omega, T_i\}$. However, to calculate the associated heat transfer rate given by $k_{eq,i}$ the convection heat transfer coefficient h_i must be determined. This quantity can be calculated from a knowledge of the power supplied to the heater and the temperature difference across the gap, using the defining relation for the heat transfer coefficient

$$Q_{\text{convection}} = h_i A_i (T_i - T_o)$$

where A_i is the total lateral surface area of the inner cylinder.

The correct evaluation of $Q_{\text{convection}}$ depends upon the proper treatment of the remaining modes of heat transfer, namely the radiative exchange between the two cylinders and the conduction interaction at the ends of the cylinders. In order to minimize both the conduction and radiation heat transfer, the magnitude of ΔT is kept small ($<20°C$). Furthermore, since it is difficult to insulate thermally a rotating test section from its bearings and support structure, it was decided to keep the inner cylinder at the ambient temperature and to obtain the desired value of ΔT by cooling the outer cylinder to below the ambient temperature. Since the outer cylinder is fixed, it could be easily insulated from its supports. On the other hand, since the inner cylinder is maintained at the same temperature as its supports, there is no significant temperature gradient to drive a heat loss (or gain). In operation, no more than a $\pm 5\%$ deviation from the mean temperature was measured on the inner cylinder surface, i.e. $|T_i(z) - T_i|/T_i \leqslant 0.05$, $0 < z < H$. No appreciable axial variation in surface temperature was found for the outer cylinder. It is noted that the outer cylinder cooling bath is never set below 0°C to ensure that no condensation develops (this is verified visually at the end of each run).

Having minimized the conduction effects, the evaluation of the convective heat transfer becomes

$$Q_{\text{convection}} = Q_{\text{electric}} - Q_{\text{radiation}}.$$

The radiation heat transfer is fairly simple to estimate, using the measured inner and outer cylinder tem-

perature. The radiative exchange between two long cylindrical surfaces is given by

$$Q_{\text{radiation}} = \{\sigma A_i(T_i^4 - T_o^4)\}/\{1/\varepsilon + A_i/A_o(1/\varepsilon - 1)\}$$

where σ is the Stefan–Boltzmann constant, ε the emissivity of the surfaces, A_i the lateral surface area of the inner cylinder, and A_o the lateral surface area of the outer cylinder. Using a tabulated value of $\varepsilon = 0.04$ for highly polished aluminum, the calculated radiation losses typically accounted for less than 3% of the total heat transfer, and were never greater than 5%.

UNCERTAINTY ANALYSIS

The uncertainty analysis presented in this section is based upon the methods discussed by Kline and McClintock [29, 30]. Four independent measurements are required for the completion of the experimental program. These measurements are for the following quantities: temperature, voltage, current, and rotational speed. From these measurements, the parameters of interest for each experiment can be calculated. The uncertainty associated with each measurement is discussed below.

For the range of voltages employed in this study, the voltage measurements have a maximum uncertainty of $\pm 0.5\%$ (of the reading in volts). The corresponding uncertainty in the measurements of current is $\pm 0.75\%$ (of the reading in amperes). These estimates of uncertainty are based on the manufacturer's specifications for the instruments used (John Fluke Mfg Co., Everett, Washington, Model 8050A Multimeters).

The measurements of rotational speed are made with a phototachometer (Power Instruments, Inc.). The model used has a stated accuracy of ± 1 r.p.m. This provides a maximum uncertainty of $\pm 2.0\%$ for rotational speeds above 50 r.p.m. for lower rotational speeds, where the relative uncertainty of the measurements is larger, the rotational speed is determined by direct visual observation (with a digital stopwatch) in order to maintain a maximum uncertainty level of $\pm 2.0\%$.

The individual temperature measurements are estimated to have an uncertainty of ± 0.2°C. This value was determined after performing a careful calibration of the temperature measuring system. Each thermocouple was individually calibrated, using an ice–water bath and boiling water as known references.

In addition to the experimental measurements, the physical dimensions of the experimental apparatus are required. These dimensions have all been determined to within a tolerance of ± 0.001 in. (25.4 μm). Furthermore, the fluid properties are also required. It has been assumed that there is negligible uncertainty in those values, which have been taken from standard sources of reference (e.g. National Bureau of Standards (U.S.) Circular 564, "Tables of Thermal Properties of Gases", 1955).

The propagation of these uncertainties into the results was subsequently evaluated, and was found to be: $Gr \pm 7.1\%$, $Re \pm 2.0\%$, $\sigma \pm 7.6\%$, and $k_{eq,i} \pm 7.1\%$.

RESULTS

Global measurements

In this section, global measurements of the mean heat transfer rates for various values of the Grashof and Reynolds numbers are presented for three different radius ratios. All experimental measurements are for the inner cylinder. The first set of data considered is for the case $\eta = 0.437$ (Fig. 3), the second is for $\eta = 0.565$ (Fig. 4), while the third is for $\eta = 0.656$ (Fig. 5). All of these annuli fall within the wide-gap category. A common behavior is observed in all cases, with the data following a power-law trend in the forced convection region.

For each set of experiments, the heat transfer rates $k_{eq,i}$ corresponding to different Grashof numbers Gr for the natural convection flows (no rotation) were first measured. These data are used to provide a baseline from which to compare and determine the effects of rotation on the heat transfer mechanism at various values of Gr. After a natural convection baseline was established, experiments were run to evaluate the effects of rotation of the inner cylinder on the heat transfer mechanism.

In Figs. 3–5, the heat transfer rate is shown as a function of the Reynolds number for various values of Gr. The abscissa is chosen to be Re^2 rather than Re, so that a direct comparison with σ can be made. It is observed that the heat transfer rate is relatively constant up to a certain critical value of the Reynolds number, above which it increases as a power of Re. Since a power-law trend is observed, the data are

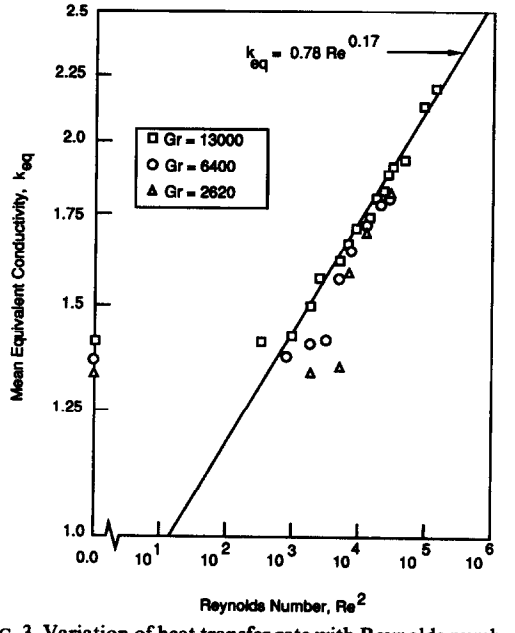

FIG. 3. Variation of heat transfer rate with Reynolds number for different Grashof numbers, with $\eta = 0.437$.

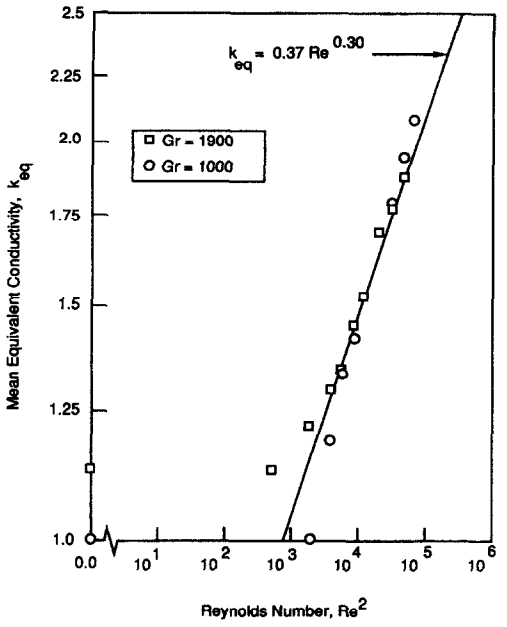

FIG. 4. Variation of heat transfer rate with Reynolds number for different Grashof numbers, with $\eta = 0.565$.

plotted on a logarithmic scale. In all three cases, the data approach an asymptote in the forced convection region

$$k_{eq,i} = 0.78Re^{0.17} \quad (\eta = 0.437)$$

$$k_{eq,i} = 0.37Re^{0.30} \quad (\eta = 0.565)$$

and

$$k_{eq,i} = 0.22Re^{0.36} \quad (\eta = 0.656).$$

The nature of the transitions to the forced-convection regime is similar for all sets of experiments. The initial increases in the heat transfer rates occur near a critical Reynolds number roughly corresponding to $\sigma \approx 1$. It is noted that the critical value of σ increases slightly as Gr is increased for a given radius ratio. This is attributed to a stronger natural convection flow being established prior to the first transition, which tends to create an axial variation in the inner cylinder surface temperature. This allows the formation of Taylor vortices at slightly lower speeds of rotation. For a more thorough discussion of this effect, see ref. [25].

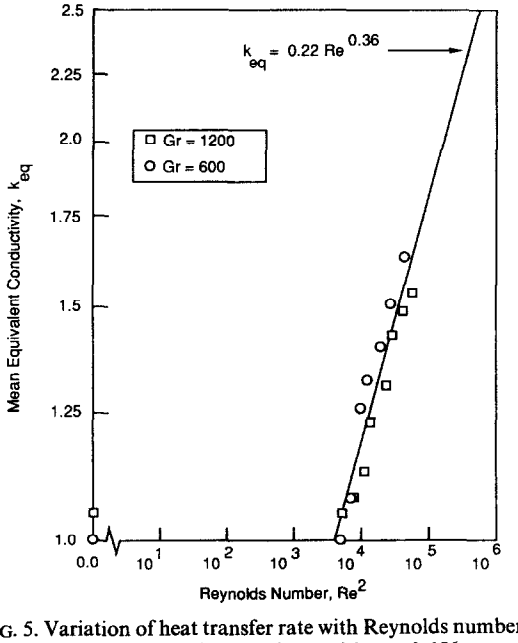

FIG. 5. Variation of heat transfer rate with Reynolds number for different Grashof numbers, with $\eta = 0.656$.

As Re increases beyond the critical value, the measurements quickly reach their asymptotic values. This is indicative of a transition from a laminar flow with no vortices to a Taylor-vortex dominated regime. The secondary flow greatly assists the transport of heat throughout the gap, and the corresponding increase in the heat transfer rate is large. The secondary flow pattern rapidly becomes fully established, and further increases in speed only increase the vigor of the flow. Thus, the data rapidly approach the power-law asymptote. No further transitions in the flow were found within the experimental range of rotational speeds.

A comparison of the heat transfer correlations for the three different radius ratios reveals that the exponent of the Reynolds number increases with η, while its coefficient decreases with η. The reason for this is that the heat transfer in the forced convection regime is accomplished through the action of the Taylor cells. As Re is increased for any particular value of η, the wave number remains fairly constant, with the cells increasing in vigor. As η is increased (i.e. the relative gap width is decreased), a greater number of Taylor cells emerge for any given annulus length. Thus, the effectiveness of the heat transfer mechanism is increased as η increases, and results in a larger exponent in the power-law relationship.

Four of the studies discussed previously have also proposed power-law relations for the heat transfer in a rotating annulus in the forced convection regime [10–13]. Bjorklund and Kays [10] considered four different radius ratios, all in the narrow range $0.8026 < \eta < 0.9488$. They did not observe any significant difference in the heat transfer relationship with varying η in this small range. If their data are averaged, the relationship

$$k_{eq} = 0.10Re^{0.5}$$

can be inferred, with $\eta = 0.8901$. This is in agreement with the trend observed in the present study. Gazley [11] also proposed a relationship of the form

$$k_{eq} = c(Re)^{0.8}.$$

In his study, the radius ratios used were $\eta = 0.9044$ and 0.9930, but a direct comparison of his data to the present study could not be made. In any event, the trends observed are supported by his study.

In the study by Aoki *et al.* [12], the effects of Prandtl number on the heat transfer were also considered. They proposed a heat transfer relation of the form

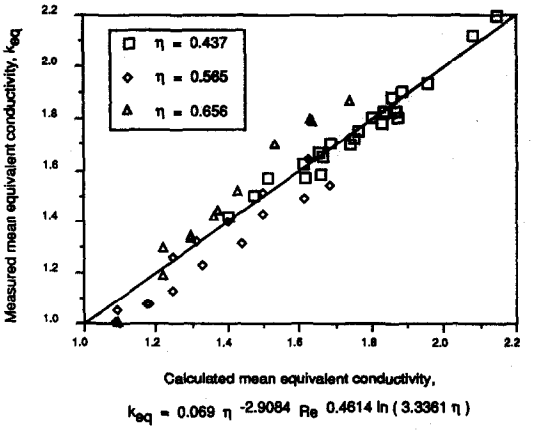

FIG. 6. Correlation of heat transfer with Reynolds number and radius ratio.

$$Nu = 0.22\, Ta^{0.25} Pr^{0.3}$$

with a Taylor number defined as $Ta = \Omega^2 R_i d^3/(\nu/F_g)$, where F_g is a geometrical factor dependent on η. Thus, while they have considered the radius ratio to have an effect on the coefficient in the power-law equation, they have neglected its effect on the exponent of *Re*. Finally, the study by Tachibana *et al.* [13] also considers Prandtl number effects, but as with Aoki *et al.*, they do not fully account for the radius ratio effects by including them explicitly in their correlation.

In Fig. 6, the results from all three radius ratios considered in this study are correlated and the following relationship is proposed:

$$k_{eq} = 0.069\, \eta^{-2.9084}\, Re^{0.4614 \ln(3.3361\eta)};$$

$$0.437 < \eta < 1.$$

This correlation is valid for air ($Pr = 0.7$) in the forced convection regime ($Gr^2 < Re < 400$). The measured values have a correlation coefficient of 0.97 with the above relation. To demonstrate its validity in the small-gap region, it is noted that this correlation is essentially equivalent to the one proposed by Bjorklund and Kays [10] for $\eta = 0.89$. The correlations proposed by Aoki *et al.* [12] and Tachibana *et al.* [13] are also consistent with the one proposed for $Pr = 0.7$.

The logarithmic dependence on η of the exponent for *Re* is not entirely unexpected. Indeed, the definition of the mean equivalent conductivity k_{eq} contains the term ln (η). This dependence arises from the cylindrical geometry. The conduction heat transfer through an annulus is easily calculated, and is given by $q = 2\pi k(T_o - T_i)/\ln(\eta)$. The action of the Taylor vortices can be likened to an enhancement of the effective thermal conductivity. This increased efficiency is reflected in the exponent of *Re*, as discussed above.

Flow visualization studies

Flow visualization has traditionally had an important role in the field of fluid mechanics and heat transfer. Visualization studies always yield valuable qualitative insight, and oftentimes quantitative results can also be obtained. One of the most interesting problems to study using visualization techniques is the Taylor problem, because of the striking nature of the transition to the regularly spaced toroidal vortices. Most of the early studies of the Taylor problem included at least some visualization results. No visualization studies have been conducted, however, for the mixed convection Taylor flows where the inner cylinder is heated.

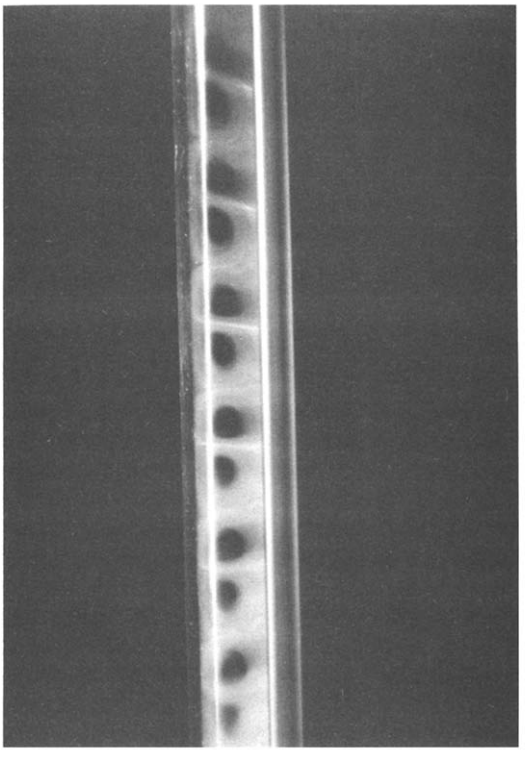

FIG. 7. Visualization of flow in vertical annulus with $Gr = 7000$, $\sigma = 0.04$.

In all of the results presented below, only one half of the annulus cross-section (in the r–z plane) is shown, with the inner cylinder on the right. It is also noted that the total width of the annulus in these results is 1.6 cm. The photographs taken are of the middle 16 cm of the annulus.

In the classic Taylor-vortex flow with a rotating inner cylinder, evenly spaced pairs of counter-rotating cells develop above a critical speed of rotation. Figure 7 shows the flow with $Gr = 7000$ and $\sigma = 0.04$. The cellular nature of this flow is clearly evident. The wave number measured from the photographs for this flow is $k = 6.4$, where k is measured in units of R_o, the outer cylinder radius. This value agrees substantially with the values reported by Chandrasekhar [31] for the isothermal case ($\sigma = 0$). At this relatively low level of buoyancy, little distortion is observed and the cells retain their fairly regular appearance. It is also observed that the centers of each pair of counter-rotating cells are closer to each other than to their

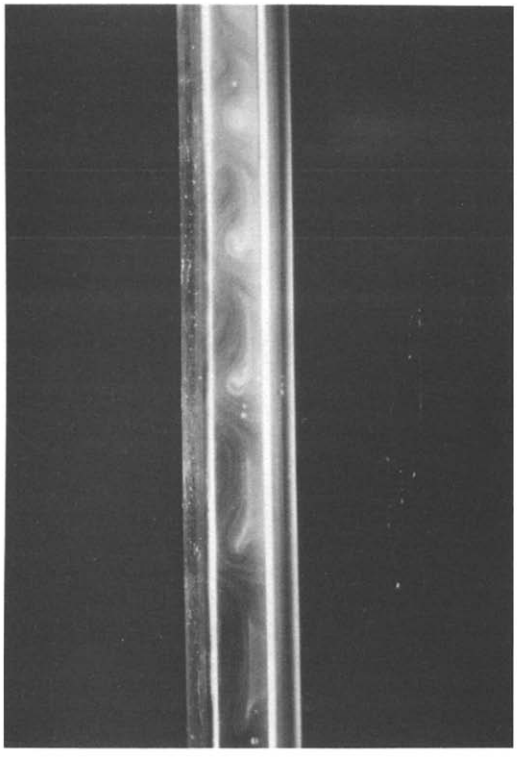

FIG. 8. Visualization of flow in vertical annulus with $Gr = 3260$, $\sigma = 0.13$.

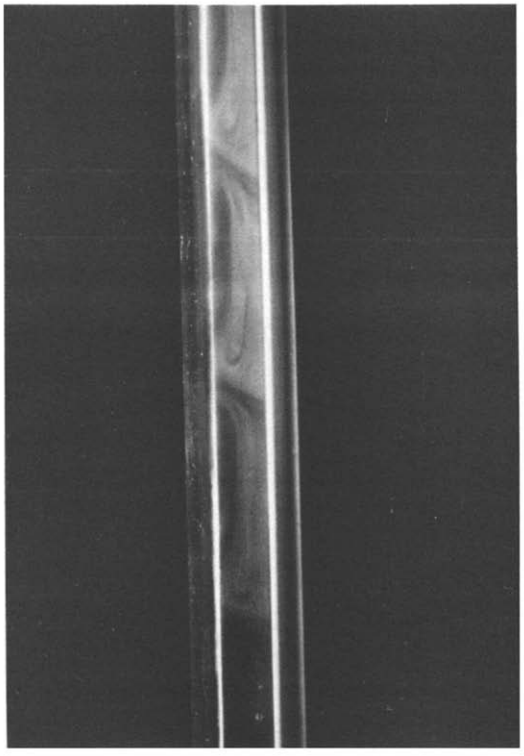

FIG. 9. Visualization of flow in vertical annulus with $Gr = 4545$, $\sigma = 0.18$.

neighbors. This phenomenon has also been reported by Snyder [19].

A 'matched' pair of cells is defined by the direction of the flow between them; for the normally occurring Taylor-cell modes, the direction of flow between each pair of cells is from the inner cylinder to the outer. In Fig. 7, the interface between each pair of cells is distinguished by a thin, dense line of smoke. The other interface, between the two cells belonging to different 'matched pairs', is not nearly as distinct. This is because the flow is more vigorous at the interface between the 'matched' pairs, and the smoke has less time to diffuse to the interior of the cells. This is consistent with their centers being closer together. On the other hand, the opposite interface is less vigorous, and the smoke diffuses inward, blurring the distinction between those adjacent cells.

The remaining figures (Figs. 8–10) show the progression of the flow as the relative amount of buoyancy is increased in the mixed convection regime (i.e. for increasing σ). It is emphasized that the results presented are largely qualitative in nature, and are not intended as an exact measure of the stability limits of the various flow regimes. Rather, the nature of the flow structure in the mixed convection regime is of primary interest. Also, the nature of the flows is determined completely by σ in the range of Gr and Re studied. That is, the same behavior was observed whether Re was held constant and Gr was increased, or Gr was held constant and Re decreased. Thus, since different combinations of Re and Gr yielding the same

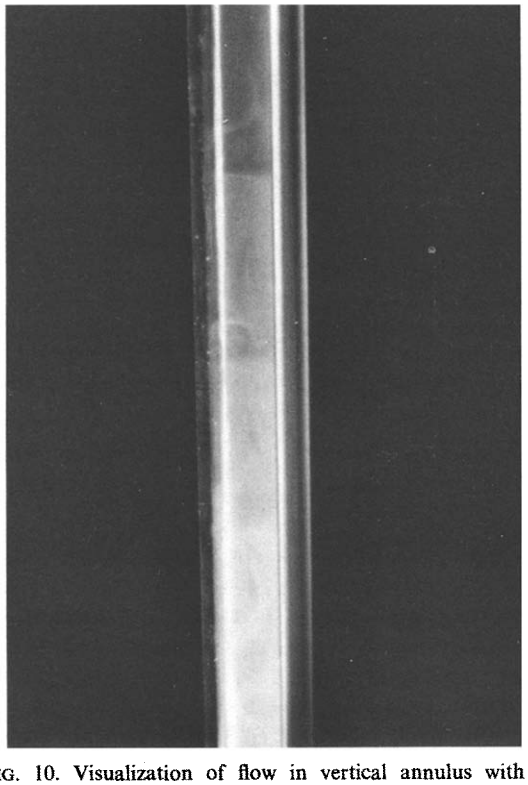

FIG. 10. Visualization of flow in vertical annulus with $Gr = 17\,775$, $\sigma = 0.3$.

value of σ produced photographs of different quality, Re and Gr were chosen to provide the sharpest images for a desired value of σ.

As σ is increased from $\sigma = 0$ to 0.1, a very slight distortion of the Taylor cells is observed, in which the upper cell in each pair has become somewhat larger than its counterpart. At this value of σ, the buoyancy is beginning to exert a stronger influence on the flow, by assisting the upward flow of air along the heated inner cylinder surface while impeding the downward flow in the counter-rotating pair. With further increases in buoyancy, an interesting phenomenon is observed. The distorted Taylor cells are noticed to travel up the annulus. This optical illusion is caused by the formation of a spiral flow, shown in Fig. 8. With further increases in σ, the spiral form becomes larger, and its appearance is much the same as a 'barber-shop pole'. This flow is shown in Fig. 9. The cellular pattern within the spiral consists of a fairly stagnant region along the outer cylinder, with a large region of upflow adjacent to the heated inner surface.

As the increase in buoyancy is continued, the spiral form becomes unstable, with a stronger region of circulation developing adjacent to the outer cylinder. Eventually, two distinct regions of circulation re-emerge and the flow once again becomes axisymmetric. In this flow (shown in Fig. 10), it is observed that each pair of counter-rotating Taylor cells is considerably distorted, consisting of a large cell underneath of a much smaller cell. The spiral form of flow is observed to be a transitory form between the distorted Taylor-cell modes and the nearly isothermal flow patterns, and occurs over a very small range of σ, which is approximately $0.1 < \sigma < 0.3$. As σ is increased above $\sigma \approx 0.3$, the cellular structure is replaced by the formation of one large toroidal cell, typical of the natural convection flow.

CONCLUSION

It is observed that the qualitative behavior of the mixed convection flows occurring within vertical annular enclosures is entirely dependent upon the value of σ for the range of experimental parameters considered. For values of $\sigma > 10$, the buoyancy forces dominate the flow, which strongly resembles the natural convection case. Similarly, for values of $\sigma < 0.01$, the rotational forces are predominant, and the flow approaches the isothermal, Taylor–Couette situation. In the range $0.01 < \sigma < 10$, both the buoyancy and the rotational forces affect the flow characteristics, with a transition between the respective flow regimes occurring near $\sigma \approx 1$. Specifically, the form of the secondary flows occurring as σ is decreased below unity consists of a cellular structure which is periodic in the axial direction. In the narrow range $0.1 < \sigma < 0.3$, this cellular structure is replaced by a spiral form of flow, which in turn gives rise to a new, axisymmetric cellular flow with continued decreases in σ. The physical appearance of the secondary flows is affected by buoyancy, until a value of $\sigma \approx 0.01$ is reached with increasing rotational speeds. Below this value of σ, the cell pattern remains unchanged, although the secondary flow increases in vigor. These results are consistent with those of the numerical studies cited previously [23–25].

The action of the secondary flows on the heat transfer characteristics of the rotational systems is significant. Until the critical value of $\sigma \approx 1$ is reached with increasing rotation (or decreasing buoyancy), the heat transfer rates remain fairly constant, at the value corresponding to the natural convection limit. With the onset of the hydrodynamic instabilities, however, a sudden and rapid rise in the heat transfer rates occurs. As the secondary flows become fully developed, the heat transfer rates for all buoyancy levels approach a common asymptote (for a given geometry), which can be described by a power-law relationship. These heat transfer rates have been correlated, and are presented as functions of the Reynolds number and radius ratio. It is observed that a greater augmentation of the heat transfer rate with increasing Reynolds number is obtainable as the relative gap width becomes narrower (i.e. for increasing values of the radius ratio η).

Acknowledgement—The authors would like to acknowledge support provided by National Science Foundation Grant CBT-8712218.

REFERENCES

1. F. Kreith, Convection heat transfer in rotating systems. In *Advances in Heat Transfer* (Edited by T. F. Irvine and J. P. Hartnett), Vol. 5, pp. 129–250. Academic Press, New York (1968).
2. A. B. Strong and L. Carlucci, An experimental study of mass transfer in rotating Couette flow with low axial Reynolds numbers, *Can. J. Chem. Engng* **54**, 295–298 (1976).
3. H. G. Wood (Editor), *Proc. Fifth Workshop on Gases in Strong Rotation*, Charlottesville, Virginia (1983).
4. P. H. Singer, Techniques of low pressure chemical vapor deposition, *Semiconductor Int.* 72–77 (May 1984).
5. H. P. Greenspan, *The Theory of Rotating Fluids*. Cambridge University Press, London (1968).
6. R. C. DiPrima and H. L. Swinney, Instabilities and transition in flow between concentric rotating cylinders. In *Hydrodynamic Instabilities and the Transition to Turbulence* (Edited by H. L. Swinney and J. P. Gollub), pp. 139–180. Springer, Berlin (1985).
7. P. D. Weidman and G. Mehrdadtehranfar, Instability of natural convection in a tall vertical annulus, *Physics Fluids* **28**, 776–787 (1985).
8. J. Kaye and E. C. Elgar, Modes of adiabatic and diabatic fluid flow in an annulus with an inner rotating cylinder, *J. Heat Transfer* **80**, 753–765 (1958).
9. K. M. Becker and J. Kaye, Measurements of diabatic flow in an annulus with an inner rotating cylinder, *J. Heat Transfer* **84**, 97–105 (1962).
10. I. S. Bjorklund and W. M. Kays, Heat transfer between concentric rotating cylinders, *J. Heat Transfer* **81**, 175–186 (1959).
11. C. Gazley, Heat transfer characteristics of the rotational and axial flow between concentric cylinders, *J. Heat Transfer* **80**, 79–90 (1958).
12. H. Aoki, H. Nohira and H. Arai, Convective heat trans-

fer in an annulus with an inner rotating cylinder, *Bull. J.S.M.E.* **10,** 523–532 (1967).
13. F. Tachibana, S. Fukui and H. Mitsumura, Heat transfer in an annulus with an inner rotating cylinder, *Bull. J.S.M.E.* **3,** 119–123 (1960).
14. F. Tachibana, S. Fukui and H. Mitsumura, Convective heat transfer of the rotational and axial flow between two concentric cylinders, *Bull. J.S.M.E.* **7,** 385–391 (1964).
15. K. M. Becker and J. Kaye, The influence of a radial temperature gradient on the instability of fluid flow in an annulus with an inner rotating cylinder, *J. Heat Transfer* **84,** 106–110 (1962).
16. Y. T. Fung and U. M. Kurzweg, Stability of swirling flows with radius dependent density, *J. Fluid Mech.* **72,** 243–255 (1975).
17. J. Walowit, S. Tsao and R. C. DiPrima, Stability of flow between arbitrarily spaced concentric cylindrical surfaces, including the effect of a radial temperature gradient, *J. Appl. Mech.* **31,** 585–593 (1964).
18. H. A. Snyder and S. K. F. Karlsson, Experiments on the stability of Couette motion with a radial thermal gradient, *Physics Fluids* **7,** 1696–1706 (1964).
19. H. A. Snyder, Experiments on the stability of two types of spiral flow, *Ann. Phys.* **31,** 292–313 (1965).
20. S. K. F. Karlsson and H. A. Snyder, Observations on a thermally induced instability between rotating cylinders, *Ann. Phys.* **31,** 314–324 (1965).
21. E. M. Withjack and C. F. Chen, An experimental study of Couette instability of stratified fluids, *J. Fluid Mech.* **66,** 725–737 (1974).
22. S. R. M. Gardiner and R. H. Sabersky, Heat transfer in an annular gap, *Int. J. Heat Mass Transfer* **21,** 1459–1466 (1978).
23. K. S. Ball and B. Farouk, On the development of Taylor vortices in a vertical annulus with a heated rotating inner cylinder, *Int. J. Numer. Meth. Fluids* **7,** 857–867 (1987).
24. K. S. Ball and B. Farouk, Numerical studies of mixed convection flows in the annulus between vertical concentric cylinders with rotating inner cylinder. In *Proc. Eighth Int. Heat Transfer Conf.*, San Francisco (Edited by C. L. Tien, V. P. Carey and J. K. Ferrell), pp. 435–440. Hemisphere, Washington, DC (1986).
25. K. S. Ball, Mixed convection heat transfer in rotating systems. Ph.D. Thesis, Drexel University (June 1987).
26. K. S. Ball and B. Farouk, Bifurcation phenomena in Taylor–Couette flow with buoyancy effects, *J. Fluid Mech.* **197,** 479–501 (1988).
27. J. A. Cole, Taylor-vortex instability and annulus-length effects, *J. Fluid Mech.* **75,** 1–15 (1976).
28. K. S. Ball and B. Farouk, A microprocessor based data acquisition system for thermo-fluid laboratories, *Rev. Scient Instrum.* **58,** 657–659 (1987).
29. S. J. Kline, The purposes of uncertainty analysis, *J. Fluids Engng* **107,** 153–160 (1985).
30. S. J. Kline and F. A. McClintock, Describing uncertainties in single-sample experiments, *Mech. Engng* **75,** 3–8 (1953).
31. S. Chandrasekhar, *Hydrodynamic and Hydromagnetic Stability*. Dover, New York (1981).

ETUDE EXPERIMENTALE DU TRANSFERT DANS UN ESPACE ANNULAIRE VERTICAL AVEC CYLINDRE INTERIEUR TOURNANT

Résumé—On présente les résultats d'une étude expérimentale des écoulements convectifs dans un espace annulaire entre cylindres concentriques. Le cylindre intérieur est tournant et chaud, tandis que l'autre est immobile et froid. Des plans horizontaux immobiles ferment la cavité. Le fluide de travail est l'air. On s'intéresse aux flux de chaleur qui sont intimement liés à la structure du champ des vitesses. Dans les systèmes tournants, l'existence d'instabilités hydrodynamiques peut conduire à une variété d'écoulements secondaires. A chaque transition dans l'écoulement, les mécanismes de transport sont altérés et il en résulte des changements dans les transferts de chaleur et de quantité de mouvement. On conduit des expériences pour déterminer l'interdépendance des mécanismes de transfert de chaleur et des structures des écoulements secondaires. On fait une étude paramétriques du flux moyen de chaleur à travers l'espace annulaire, et aussi une étude qualitative (par visualisation à l'aide de fumée) des écoulements secondaires. On obtient une description de la transition depuis le régime dominé par le flottement jusqu'à celui dominé par la rotation. Une formule est obtenue pour le flux de chaleur en fonction du nombre de Reynolds rotationnel et du rapport des rayons, dans le cadre de la convection forcée.

EXPERIMENTELLE UNTERSUCHUNG DES WÄRMEÜBERGANGS IN EINEM ZYLINDRISCHEN VERTIKALEN RINGRAUM MIT ROTATION DES INNEREN ZYLINDERS

Zusammenfassung—Die Ergebnisse einer experimentellen Untersuchung der in einem Ringspalt zwischen konzentrischen vertikalen Zylindern auftretenden Konvektionsströmung werden vorgestellt. Der innere rotierende Zylinder wird beheizt, während der äußere unbewegliche Zylinder gekühlt wird. Feste horizontale Endplatten werden als Begrenzung des Ringraumes verwendet; damit wird ein abgeschlossener Raum begildet. Das Arbeitsmedium ist Luft. Von besonderem Interesse ist die genaue Berechnung der Wärmeübertragung, welche eng an die Struktur des Strömungsfeldes gekoppelt ist. In rotierenden Systemen kann die Existenz von hydrodynamischen Instabilitäten zu einer Vielzahl von Sekundärströmungen führen, die so zahlreich sind wie die Parameter, die das System beschreiben. Mit jeder Änderung der Strömungsform werden die Transportmechanismen verändert; dies verursacht gewöhnlich einen auffallend veränderten Wärme- und Impulstransport. Experimente zur Bestimmung der gegenseitigen Abhängigkeit zwischen dem Wärmeübertragungsmechanismus und der Struktur der Sekundärströmungen werden durchgeführt. Im besonderen wird eine Parameterstudie für die mittlere Wärmeübertragung im Ringspalt ausgeführt, desgleichen eine qualitative Untersuchung (mittels der Anwendung von Rauchverfahren zur Sichtbarmachung) der Charakteristiken der Sekundärströmung in dem rotierenden System. Die Ergebnisse gehen ein in eine qualitative Beschreibung des Übergangs von einem durch dynamische Auftriebskräfte beherrschten zu einem durch Rotation beherrschten Strömungszustand. Im Bereich der erzwungenen Konvektion erhält man eine Korrelation für die Wärmeübertragung als Funktion der durch die Rotation erzeugten Reynolds-Zahl und des Radienverhältnisses.

ЭКСПЕРИМЕНТАЛЬНОЕ ИССЛЕДОВАНИЕ ТЕПЛОПЕРЕНОСА В ВЕРТИКАЛЬНОМ КОЛЬЦЕВОМ КАНАЛЕ С ВРАЩАЮЩИМСЯ ВНУТРЕННИМ ЦИЛИНДРОМ

Аннотация—Представлены результаты экспериментального исследования конвективных потоков в кольцевом зазоре между концентрическими вертикальными цилиндрами. Внутренний цилиндр вращается и нагревается, а внешний неподвижен и охлаждается. Неподвижные горизонтальные торцевые пластины замыкают кольцевой канал, тем самым образуя полость. Рабочей текучей средой является воздух. Особый интерес представляет точное описание интенсивности теплопереноса, тесно связанной со структурой поля течения. Наличие гидродинамической неустойчивости во вращающихся системах может привести при варьировании параметров, описывающих систему, к появлению различных вторичных течений. С каждой перестройкой течения меняются и механизмы переноса, в результате чего обычно значительно изменяются также интенсивности переноса тепла и импульса. Проведены эксперименты по определению взаимосвязи между механизмом теплопереноса и структурой вторичных течений. В частности, исследована параметрическая зависимость средней интенсивности теплопереноса через кольцевой зазор, а также изучены (методом дымовой визуализации течения) качественные характеристики вторичных течений во вращающейся системе. Результаты представляют качественное описание перехода от режима с преимущественно свободноконвективным течением к режиму с доминирующим течением, обусловленным вращением. Интенсивность теплопереноса представлена как функция вращательного числа Рейнольдса и отношения радиусов для предельного случая свободноконвективного режима.